Tellus (2008), 60B, 318–329
Printed in Singapore. All rights reserved

TELLUS

Analysis of one year of Ion-DMPS data from the SMEAR II station, Finland

By STÉPHANIE GAGNÉ[1]*, LAURI LAAKSO[1], TUUKKA PETÄJÄ[1,3], VELI-MATTI KERMINEN[2] and MARKKU KULMALA[1], [1]*Department of Physical Sciences, University of Helsinki, P. O. Box 64, FI-00014, Helsinki, Finland;* [2]*Finnish Meteorological Institute, Erik Palmenin Aukio 1, FI-00101, Helsinki, Finland;* [3]*Earth and Sun Systems Laboratory, Atmospheric Chemistry Division, National Center for Atmospheric Research, PO Box 3000, Boulder, CO 80307-5000, USA*

(Manuscript received 10 October 2007; in final form 18 February 2008)

ABSTRACT

In this paper, we investigate the participation of ion-induced nucleation in atmospheric new-particle formation. We present one year of Ion-DMPS data from the SMEAR II station in Hyytiälä, southern Finland (22 September 2005 to 22 September 2006). We measured continuously the concentrations of ions in ambient and charge equilibrated air in seven size bins over a diameter range 3–15 nm. All new-particle formation event days were classified according to observed particle charging states and analysed based on a new theoretical tool by which the measured charging states can be extrapolated down to smaller particle sizes. We investigated the contribution of ion-induced nucleation for both positively and negatively charged particles. The median contribution of ion-induced nucleation at 2 nm during the one year of measurements was around 6.4% with a median absolute deviation (MAD) of 2.0%,. The smallest contribution was 1.7% (MAD = 1.6%) whereas the maximum was 16.5% (MAD = 2.2%). We also analysed the data on a seasonal basis and found the largest contribution of ion-induced nucleation during summer (7.6%) and lower during the rest of the year (4.9%).

1. Introduction

Aerosol particles influence the Earth's radiation balance directly by scattering and absorbing solar and terrestrial radiation and indirectly by acting as cloud condensation nuclei (e.g. Chung et al., 2005; Lohmann and Feichter, 2005; Penner et al., 2006). In addition to this, aerosol particles have adverse effect on human health and deteriorate visibility in polluted environments (Donaldson et al., 1998; Pope and Dockery, 2006). The amount and properties of atmospheric aerosol particles is tied strongly with various natural and anthropogenic sources. One clearly important source in this respect is atmospheric new-particle formation (e.g. Kulmala et al., 2004; Spracklen et al., 2006).

Depending on the location and prevailing conditions, new atmospheric aerosol particles may be produced from different precursor vapours and by different mechanisms (Kulmala, 2003). The very initial steps of atmospheric new particle formation may involve ions or take place entirely via neutral pathways. The contribution of ion-induced nucleation to the overall new-particle formation rate has remained unclear. Some studies suggest that this contribution could be substantial or even dominant (Yu and Turco, 2001; Yu et al., 2006), whereas some other studies are indicative of a relatively minor contribution (e.g. Iida et al., 2006; Vana et al., 2006; Laakso et al., 2007).

One way to track down the importance of ion-induced nucleation based on field measurements is use the concept of 'charging state' (e.g. Laakso et al., 2007). The charging state is the extent to which a particle population is charged compared with the corresponding stationary-state value. Technically, this quantity is calculated as the ratio between the number concentration of charged particles in a certain particle population and the stationary-state concentration of charged particles in the same particle population. Knowledge about the charging state of particles close to the sizes at which they nucleate provides information on whether ion-induced nucleation was participating or not in the new-particle formation event. Kerminen et al. (2007) derived an approach by which measured charging states of nucleation mode particles can be extrapolated down to smaller particle sizes using a simple mathematical formula. The approach is based on the idea that a growing particle population is able to maintain some information about its original charging state during the growth. In some cases, this information is lost before

*Corresponding author.
e-mail: stephanie.gagne@helsinki.fi
DOI: 10.1111/j.1600-0889.2008.00347.x

particles reach detectable sizes, making it impossible to distinguish between neutral and ion-induced nucleation.

The particle charging state can be measured using different combinations of ion-spectrometers and Differential or Scanning Mobility Particle Sizers (DMPS; Vana et al., 2006). The observation of ion-induced nucleation has recently been made possible by the development of new ion spectrometers. The Ion-DMPS is a relatively new device that measures directly the particle charging state (Mäkelä et al., 2003; Laakso et al., 2007). In this work, we present one full year of Ion-DMPS data analysed using the formula introduced by Kerminen et al. (2007). The cases for which this formula can, and cannot, be used to extrapolate the charging state to smaller particle sizes are discussed. Moreover, we present a seasonal trend analysis as well as a classification of event (ion-induced and not) and non-event days as a function of the time of year.

2. Instrumentation and methods

2.1. Ion-DMPS

The data presented in this work was measured with an Ion-DMPS between 22 September 2005 and 22 September 2006. The measurements took place in Hyytiälä, SMEAR II measurement station (61°51′N, 24°17′E, 181m asl), Finland. The Ion-DMPS (Laakso et al., 2007) is composed of a DMA (length 0.109 m, Winklmayr et al., 1991) and a CPC (TSI 3025, Stolzenburg and McMurry, 1991) along with a bipolar charger (neutralizer, Ni-63, Reischl et al., 1996) that can be switched on and off. The DMA's polarity can also be switched between negative and positive potential allowing the Ion-DMPS to work in four modes: 1) negative charge equilibrated (bipolar charger on), 2) negative ambient (bipolar charger off), 3) positive charge equilibrated and 4) positive ambient. The sample is first charge equilibrated (or not) and then goes to the DMA, which selects only positively (or negatively) charged particles of a specific size to be counted downstream by the CPC (see Fig. 1). For this data set, the Ion-DMPS was measuring between 3 and 15 nm in seven size bins. The minimum concentration included in the analysis was 0.1 cm^{-3}.

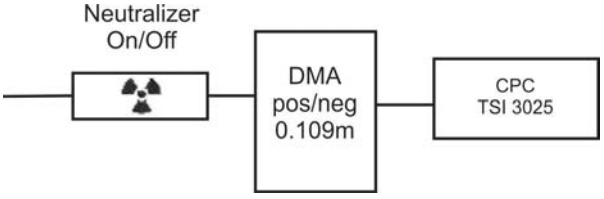

Fig. 1. In the Ion-DMPS, the air sample is first led to a bipolar charger (neutralizer, Ni-63), which can be either on or off. The particles are then size and charge segregated by a Differential Mobility Analyzer (DMA, 0.109 m). The charged particles continue to the Condensation Particle Counter (CPC, TSI 3025) where the charged particles are counted.

2.2. Method of analysis

Nucleation events are characterized by formation of new particles at sizes of the order of 1–2 nm (nucleation mode) and their subsequent growth to sizes of a few tens of nanometres. The analysis of one full year allows us to see if there were peaks or minima in the contribution of ion-induced nucleation during the year. We started the analysis by classifying the days into different categories based on whether new-particle formation took place, after which the event days were further analysed with respect to their initial charging state.

The method for classifying the new-particle formation events was based on that developed by Dal Maso et al. (2005) for DMPS data, but the nature of our data did not allow its use without modifications. Indeed, the Ion-DMPS provides the number concentration of ions with varying detection efficiencies that depend on the particle size, whereas the DMPS shows the total (ions and neutral) particle number concentration. Hence, the classification used with the Ion-DMPS was different but strongly inspired from that described by Dal Maso et al. (2005). All the days in the analysed period were first classified into four categories: non-event, event, undefined and bad/no data. The non-event day category includes all the days for which no formation of new particles was observed. The event day category includes those days for which new particles appear at lower size bins and grow to bigger sizes during the day. The undefined day category is rather wide. It includes all days for which new particles appear at sizes larger than 4–5 nm (this is difficult to see with an Ion-DMPS because the charging efficiency for small particles is small and so are the concentrations). It also includes days in which new particles do not grow to bigger sizes or a blast of particles stays in the ambient air only for a short moment. The last category, bad/no data, includes days for which no, or only partial, data are available, or for which the event classification cannot be applied.

Newly-formed particles are expected to be charged when formed by ion-induced nucleation and electrically neutral when formed via other nucleation pathways. In both cases, the fraction of charged particles evolves gradually toward the corresponding stationary-state value as the nucleated particles grow to bigger sizes. This means that if the charging state of the smallest particles is >1, ion-induced nucleation must have been involved in the new-particle formation event. When no ion-induced nucleation has taken place, the charging state of the smallest particles should be ≤ 1. The charging state of particles larger than about a few nanometres in diameter should approach unity regardless of the nucleation mechanism.

The days categorized as event days were further classified into four classes: overcharged, undercharged steady-state and not determined, with respect to their charging state. Event days were said to be overcharged when the charging state of the first few size bins was >1 and undercharged when it was <1. The steady-state class included event days for which all the points from all the size bins were oscillating around 1. The

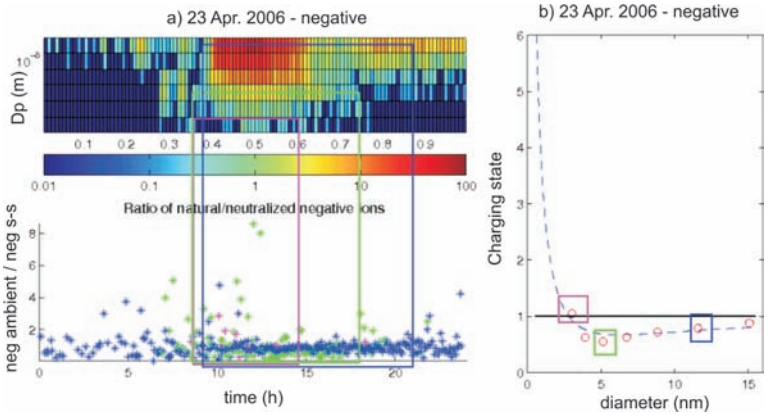

Fig. 2. (a) shows how the ratio of charged particles for ambient (natural) sample to charged equilibrated (neutralized) sample is selected for each size bin while the nucleation mode particles are crossing this size bin. The magenta colour represents 3 nm particles, green 5 nm and blue 11 nm. The coloured rectangles are there as guide for the eye to show the period when the nucleation mode crosses the size bin (chosen from the upper figure and has effect on the points taken in the lower figure for the calculation of the median charging state). In part (b), the median charging state of each size bin in the selected period—in (a)—is plotted as a function of diameter.

label 'not determined' was given to event days that could not be classified.

To differentiate between the different charging state cases, and thereby to get information about the participation of ion-induced nucleation, plotting the charging state as a function of the particle size is very useful. In this work, we calculated the median charging state of each size by considering the time period over which the growing particles were in that given size bin (Fig. 2a). The median charging state was then plotted as a function of size (Fig. 2b). The dotted line is a fit to an equation that is presented in the next paragraph.

2.3. Analytical formula for the particle charging state

A formula describing the behaviour of the charging state of a growing particle population as a function of particle size has been derived by Kerminen et al. (2007) and is given by:

$$S(d_p) = 1 - \frac{1}{K d_p} + \frac{(S_0 - 1)K d_0 + 1}{K d_p} e^{-K(d_p - d_0)}, \quad (1)$$

where

$$K = \frac{\alpha N_{\pm}^{C}}{GR}. \quad (2)$$

In eq. (1), $S(d_p)$ is the charging state of particles of the diameter d_p, S_0 and d_0 are the charging state and diameter of newly-formed particles, respectively, $N_{\pm}^{C}$ is the number concentration of ion clusters, GR is the particle growth rate and α ($\sim 1.6 \times 10^{-6}$ cm^3 s^{-1}) is the ion-ion recombination coefficient. The idea of our analysis is to extrapolate the measured charging states above 3 nm down to the sizes (d_0) at which nucleation was likely to have taken place. The resulting value of S_0 at d_0 can then be related to the contribution of ion-induced nucleation to the total nucleation rate.

Although based on detailed balance equations between ions and neutral clusters, pre-existing larger particles and condensing vapours, a number of assumptions and approximations had to be made in deriving eq. (1). Kerminen et al. (2007) performed a sensitivity analysis on the applicability of this equation and found that systematic errors in the extrapolated values of S_0 would occur under the following conditions: (1) the concentration of growing nanoparticle population is much higher than the ion cluster concentration; (2) the coagulation sink of the pre-existing particle population is exceptionally large (polluted air); (3) ion-ion recombination is an important source of neutral clusters at sizes of around d_0; (4) charged nanoparticles (nuclei) grow faster than neutral ones; (5) the ion-induced nucleation dominates the overall nucleation rate or (6) the nuclei growth rate, GR, is not constant. The conditions in our measurements were such that the points (1) and (2) listed above are not expected to cause any significant error in the extrapolated value of S_0. The same is very likely to be true in case of point (3) based on the analysis by Kulmala et al. (2007). The influence of point (4) is difficult to quantify in lack of proper experimental data. However, by relying on the analysis of Iida et al. (2006), we may estimate that this effect would cause a systematic overestimation (up to a factor of two), rather than underestimation, of the contribution of ion-induced when using eq. (1). In cases where ion-induced nucleation is the dominant nucleation mechanism, extrapolated values of S_0 become highly inaccurate, precluding quantitative estimation of this contribution. In spite of these inaccuracies, eq. (1) should unambiguously reveal whether ion-induced nucleation had been the dominant nucleation mechanism or not.

Perhaps the most serious problem when using eq. (1) is that the nuclei growth rate is unlikely to be constant. Especially, there are indications that sub-3 nm particles grow usually slower than particles >3 nm in diameter (e.g. Hirsikko et al., 2005). Kerminen et al. (2007) demonstrated that if the growth rate of sub-3 nm particles were only half of that of larger particles, typical errors (a systematic underprediction) in the extrapolated values of S_0 would be in the range 20–50% if the 'real' value of S_0 (at 1.5 nm) was in the range 1–10 and 30–70% when the 'real' value of S_0 was in the range 10–50. In lack of reliable data on sub-3 nm particle growth rates, no attempt was made here to account for this effect. We should keep in mind, therefore, that the 'real'

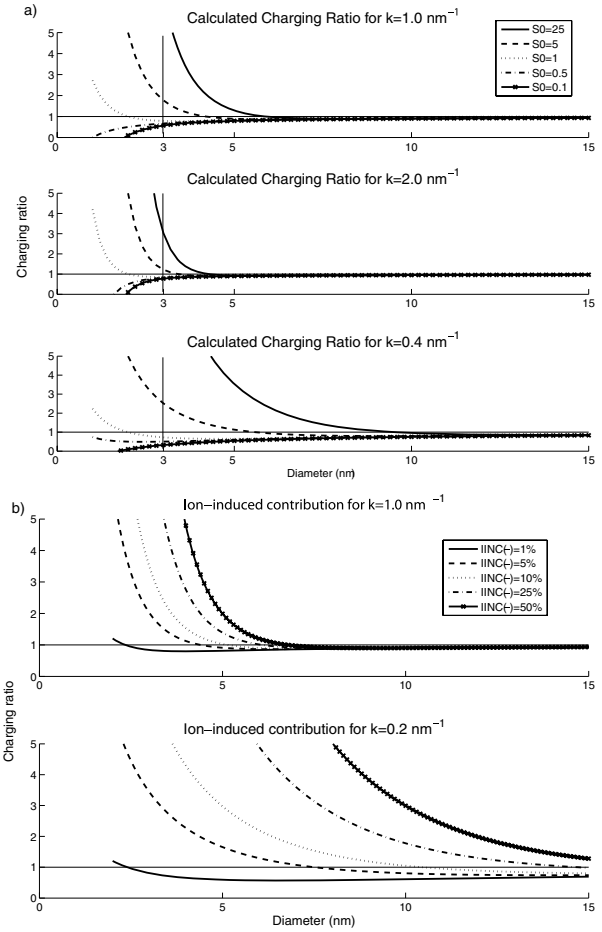

Fig. 3. (a) Equation 1 is plotted with different values of the parameters K and S_0. The initial charging state S_0 is evaluated for five different values: 25, 5, 1, 0.5 and 0.1. The top plot has $K = 1.0$ nm^{-1}, the middle one $K = 2.0$ nm^{-1} and the bottom one has a value of $K = 0.4$ nm^{-1}. Usually values of K under 1 or 1.5 nm^{-1} are considered to reflect a sufficient memory within the charging state range observed in Hyytiälä. (b) The ion-induced contribution (IIC) for negative particles only is shown for two values of K (1 and 0.2 nm^{-1}) and five values of IIC (1%, 5%, 10%, 25% and 50%).

contribution of ion-induced nucleation might be somewhat higher than that obtained by using eq. (1).

Finally, it should be noted that using eq. (1) is meaningful only in cases when the growing particle population keeps traces of its original charging state. This so-called 'memory' of the charging state is described by the parameter K. The smaller the value of K is, the longer the particle population remembers its original charging state (see Fig. 3). So, when the particle growth rate is high and the ion cluster concentration is small, the 'memory' of the charging state is at its best. On the other hand, particles growing at a low rate will reach their stationary-state charge distribution before getting to detectable sizes, as a result of which all information on their initial charging state has been lost. Figure 3b shows the curve related with their ion-induced contribution. It should be noted that even if the ion-induced contribution is only 5%, the overcharging is very apparent.

In theory, the use of eq. (1) is limited by the memory effect described above. When the memory is not long enough, all measurement data points down to 3 nm are close to the line with a charging state equal to unity. In that case, the range of parameters that can be fitted to the measured data points is very large and the 'real' behaviour at smaller particle sizes becomes impossible to be extrapolated. In practice, the most obvious cases in which this equation could not be used was when all the measured points oscillated around the line $S = 1$. In that case, there is no way to tell whether the initial charging state had been smaller or larger than unity. Another case was when all the measured data points were around the line $S = 1$, except for the smallest size bin. In such cases, the fit behaved in an unphysical manner. This could probably be improved, however, by calculating the value of K from independent measurements and limiting the K parameter to its measured value, assuming that the data point has small enough uncertainties. In most event days however, eq. (1) was applicable. Moreover, a sample of K values was calculated from independent instruments (BSMA, Tammet, 2006) for all possible event days between 13 April 2005 and 15 May 2006. The resulting minimum, median and maximum values of K were 0.26, 1.0 and 2.55 nm^{-1}, respectively. It is, therefore, improbable that under conditions typical for Hyytiälä, K would be large enough to remove entirely the signal of a very large contribution from ion-induced nucleation from the measurable size range (>3 nm). However, it is possible that mildly overcharged or undercharged events went undetected because of large values of K in those particular events.

2.4. Sensitivity to diameter at which particles are formed

A recent analysis shows that the processes initiating new-particle formation starts from sizes of around 1.5 nm (Kulmala et al., 2007). The definition of the diameter d_0 at which newly-formed particles appear, influences the extrapolated value of ion-induced contribution. To test how the initial diameter influences on charging state values, fittings have been made for two initial diameters: 1.5 and 2.0 nm (Millikan diameter). No significant difference in the parameter K has been found except for 2 and 11 d for the negatively and positively charged particles, respectively. The great majority of these days for which the parameter K differed significantly had rather high values of K, which means that the memory of the charging state faded rapidly in size. The evaluation of the ion-induced contribution is more difficult. The charged fraction is higher for bigger particles whereas the charging state tends to be higher for smaller particles in the case of overcharged events. These two differences, however, do not compensate one another. Indeed, the median ion-induced contribution was 0.6% (negative) and 0.5% (positive) more when $d_0 = 1.5$ nm compared $d_0 = 2.0$ nm. For the vast majority of events the ion-induced

contribution was higher if d_0 was 1.5 nm since the majority were overcharged events.

2.5. *Sensitivity analysis of the fitting parameter K and S_0 and charging of particles in a bipolar charger*

Since the values of the fitting parameter K and S_0 depend on exact locations of the diameter-corrected data points, it is clear that they are affected by uncertainties in measured particle diameters and corresponding charging states. To evaluate how much K and S_0 vary within the limits of the uncertainty, we generated 2000 normally-distributed points randomly around the actual measured diameter-corrected data points, and fitted those points using eq. (1). The random data points were generated within the uncertainty of the diameter and the charging state; so inside a box, normally distributed around its central point. The median absolute deviation (MAD) was found to be the most representative value for the distribution of the fitted parameters. The MAD for a distribution X is defined as follows:

$$\mathrm{MAD} = \mathrm{median}\,|X - \mathrm{median}(X)| \tag{3}$$

The MAD thus tells how much the parameters typically vary when the points are generated randomly around the measured points. It is important to remember that S_0 and K are coupled parameters, that is, they are not independent of each other. The errors observed in the values of K were small when considering the range within which K can vary, for example, a value of $K = 0.2$ nm^{-1} can have a MAD larger than itself and thus can reside between 0 and 0.4 nm^{-1}, which however doesn't alter the ion-induced contribution values.

One additional source of error, as described by Laakso et al. (2007), is an artefact introduced by the bipolar charger (observed only for negative particles). In our previous laboratory experiments, we found that the charger may increase the concentration of small, negative particles. To study the uncertainties caused by this phenomenon, we investigated the resulting potential error for each day. By assuming the worse possible conditions with regard of this phenomenon, the median error in S_0 was found to be around 43%. By considering the overall values of S_0 observed in this work, this will not significantly change our main conclusions. Moreover the worse conditions are probably much worse than the conditions in Hyytiälä because the bipolar charger can produce particles via ion-induced nucleation in polluted air. Hyytiälä is relatively clean, so this phenomenon is probably not happening in such a large extent.

3. Results

3.1. *New-particle formation event during the measurement period*

The number of event days was the highest between March and September, 2006 (Fig. 4). Typically, the event frequency in Hyytiälä peaks in spring and autumn with lower frequencies in summer and winter (Dal Maso et al., 2005). The studied year was unusual in terms of weather conditions. Indeed, the summer of 2006 was one of the driest during the last hundred years. However, a larger number of undefined events were noticed during summer in previous years with DMPS measurements (see Dal Maso et al., 2005 for classification definition). It could be thought that the lack of water in the system have helped otherwise aborted events to become fully event days. A high relative humidity has been known to prevent new formation events to happen, and relative humidity has been fairly low during the drought. An investigation of the total ion-induced contribution at 2 nm as a function of temperature and relative humidity is presented in a subsequent section.

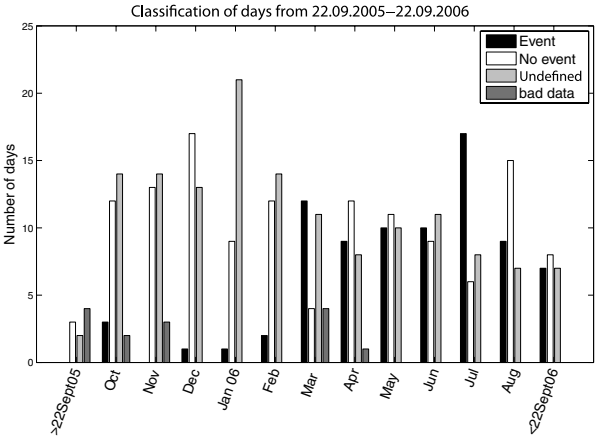

Fig. 4. This shows the classification of each day during the analysed period for each month. Note that only part of both September months are shown, which explains that the total number of days for these two month is low. During the year most of the nucleation events took place between March and September 2006.

The classification of new-particle formation events based on charging state is shown in Fig. 5. The classification was made visually by comparing the concentrations of ions from the size distribution plots. The steady-state category could not be analysed using eq. (1) due to reasons outlined in section 2.3. One can see that overcharged events were the dominant class in Hyytiälä, followed by steady-state events and finally a few clearly undercharged events. All the undercharged events were encountered in spring whereas the summer was filled with overcharged events only. In the rest of this paper, steady-state and undercharged events will be grouped together because they both suggest that no or very little ion-induced nucleation was taking place during new-particle formation. During our measurement period, we detected 81 new-particle formation events, of which 62 were overcharged, 2 were undercharged, 16 were at steady-state and 1 was not determined for the negatively charged particles. For the positively charged particles 55 events were overcharged, 6 undercharged, 15 at steady-state and 5 not determined.

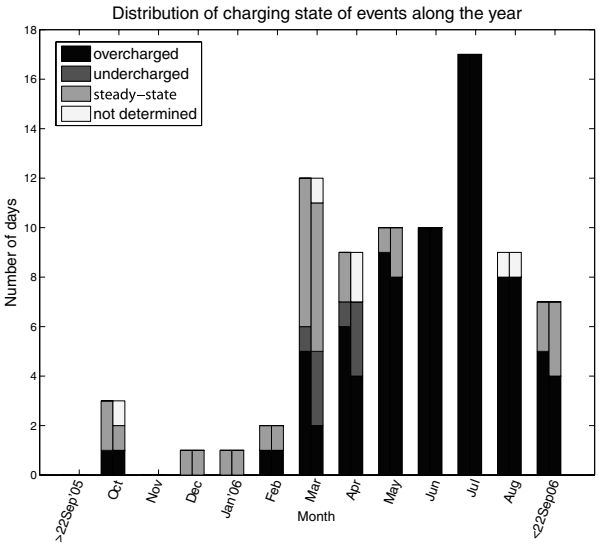

Fig. 5. The classification of event days into four categories according to their charging state. The first and second column of each month shows the classification for negatively and positively charged particles, respectively.

3.2. Contribution of ion-induced nucleation

Figure 6 shows all the measured charging states during the full year of measurements, as separated between the event and non-event days. The overall pattern of having dominantly overcharged events is apparent. Table 1 lists the values of the parameter K and initial charging state S_0 obtained from fittings into the measurement data as well as an evaluation of their sensitivity (MAD). Table 2 summarizes the statistics extracted from Table 1 for the fitting parameters K and S_0. The median values of these parameters are shown for each charging state class as well as for all classes together. It should be noted that due to the memory effects discussed in Section 2.3, new-particle formation event having lower values of K are more reliable for analyses. As a result, our later analysis will be based on cases with K having a maximum value of unity.

By assuming a stationary-state charged fraction of 0.83% for negatively charged particles and a corresponding value of 0.75% for positively charged particles at 2.0 nm (Wiedensohler, 1988; Hoppel and Frick, 1986), it is possible to calculate the ion-induced contribution during new-particle formation events. The total ion-induced contribution was calculated by adding the

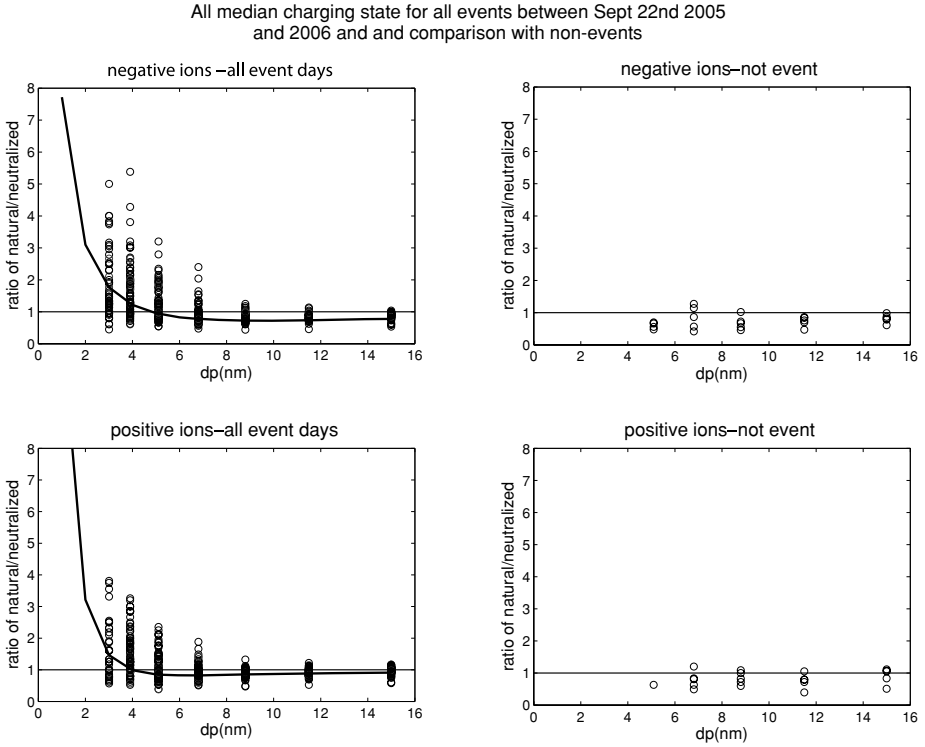

Fig. 6. All median charging state for all sizes and event days in the analysed period are shown on the left hand side of the figure for negative (up) and positive (down) ions. The same figure is show for five randomly selected non-event days for which no tendency in the charging state as a function of size can be seen. The line on the event side represents the fit of eq. (1) to the median point of each size bin (no real event). This shows that in average, during the analysed period, events were generally overcharged, implying a certain contribution of ion-induced nucleation. To understand this figure, it is important to remember that the points represent the ratio between the ambient and the charged equilibrated concentration. When particles are 5 times more charged than in stationary state the charging state is 5, on the other hand when it is 5 times less charged the charging state is 0.2.

Table 1.The event days along with the day of year, the parameter K, the initial charging state at 2 nm and extrapolated charging state at 1.5 nm along with the charging state is given for both negatively and positively charged particles

		S_0-						S_0+					
Date (dd month yyyy)	DOY	K–(nm^{-1})	MAD K–(N m^{-1})	S_0- (@ 2 nm)	MAD S_0-	(@ 1.5 nm)	ChS	$K+$ nm^{-1}	MAD $K+$ (nm^{-1})	S_0+ @ 2 (nm)	MAD S_0+	S_0+ (@1.5 nm)	ChS
4 Oct 2005	277	0.31	0.18	5.77	1.57	8.79	1	1.53	0.36	66.81	3.76	190.07	1
5 Oct 2005	278	0.59	0.28	2.86	1.06	4.72	0	0.66	0.29	2.34	1.23	3.88	0
10 Oct 2005	283	1.07	0.39	3.06	1.30	6.13	0	–	–	–	–	–	3
13 Dec 2005	347	0.42	0.24	2.45	0.91	3.76	0	–	–	–	–	–	0
27 Jan 2006	27	0.84	0.37	6.29	2.64	12.15	0	–	–	–	–	–	0
25 Feb 2006	56	0.53	0.27	2.76	1.13	4.44	1	–	–	–	–	–	1
26 Feb 2006	57	0.22	0.12	3.08	0.87	4.45	0	1.61	0.41	−8.61	5.23	−27.15	0
11 Mar 2006	70	0.56	0.25	2.97	1.33	4.86	1	1.15	0.40	6.26	1.89	13.91	3
12 Mar 2006	71	0.65	0.32	2.77	0.96	4.66	1	–	–	–	–	–	0
13 Mar 2006	72	0.88	0.36	3.17	0.85	5.91	1	0.95	0.38	0.18	0.52	−0.33	−1
14 Mar 2006	73	–	–	–	–	–	0	0.71	0.33	1.95	1.68	3.21	−1
17 Mar 2006	76	0.19	0.10	2.20	1.04	3.11	0	0.48	0.26	2.63	1.53	4.14	0
19 Mar 2006	78	0.41	0.13	2.91	1.15	4.50	1	–	–	–	–	–	1
20 Mar 2006	79	0.79	0.37	2.77	0.97	4.91	0	–	–	–	–	–	0
21 Mar 2006	80	1.20	0.56	−0.04	1.25	−1.07	−1	2.00	0.65	2.20	1.91	5.92	−1
22 Mar 2006	81	–	–	–	–	–	0	1.59	0.32	9.88	1.31	27.73	0
23 Mar 2006	82	1.40	0.46	21.97	3.52	57.79	1	–	–	–	–	–	1
24 Mar 2006	83	–	–	–	–	–	0	–	–	–	–	–	0
25 Mar 2006	84	0.36	0.22	2.10	1.56	3.12	0	–	–	–	–	–	0
16 Apr 2006	106	0.44	0.27	2.58	1.03	4.00	1	1.24	0.43	9.94	2.27	23.62	1
17 Apr 2006	107	–	–	–	–	–	−1	–	–	–	–	–	−1
20 Apr 2006	110	0.28	0.22	2.88	0.89	4.24	1	–	–	–	–	–	1
21 Apr 2006	111	–	–	–	–	–	1	0.59	0.27	3.63	2.34	6.10	1
22 Apr 2006	112	0.10	0.00	4.23	0.90	5.87	1	–	–	–	–	–	3
23 Apr 2006	113	0.32	0.14	1.45	0.59	2.07	0	0.47	0.21	0.72	1.43	0.90	−1
24 Apr 2006	114	0.31	0.15	2.35	0.82	3.46	1	0.51	0.26	3.91	1.57	6.39	1
25 Apr 2006	115	0.10	0.00	2.68	0.62	3.70	1	–	–	–	–	–	3
30 Apr 2006	120	0.22	0.11	2.00	0.75	2.84	0	0.37	0.18	0.32	1.41	0.28	−1
6 May 2006	126	0.28	0.21	4.11	1.14	6.13	1	1.21	0.37	9.23	2.42	21.55	1
8 May 2006	128	0.10	0.00	6.99	1.12	9.74	1	0.10	0.00	4.46	1.39	6.19	1
9 May 2006	129	0.10	0.00	3.61	0.72	5.00	1	0.24	0.07	4.33	1.53	6.36	1
10 May 2006	130	0.23	0.12	6.81	2.00	10.04	1	0.34	0.25	5.11	1.70	7.86	1
11 May 2006	131	0.11	0.00	3.00	0.79	4.16	1	0.22	0.11	1.40	0.99	1.95	0
14 May 2006	134	2.48	0.40	0.04	1.22	−2.76	1	0.70	0.27	8.16	2.08	14.95	1
15 May 2006	135	1.72	0.53	28.70	3.63	88.81	1	0.49	0.24	2.51	0.90	3.95	1
16 May 2006	136	0.88	0.43	1.90	1.22	3.28	0	–	–	–	–	–	0

Table 1. cont'd

		S_0-						S_0+				
Date (dd month yyyy)	DOY	$K-(nm^{-1})$	MAD $K-(N\ m^{-1})$	S_0- (@ 2 nm)	MAD S_0-	(@ 1.5 nm)	ChS	$K+\ nm^{-1}$	MAD $K+\ (nm^{-1})$	S_0+ @ 2 (nm)	MAD S_0+	S_0+ (@1.5 nm)	ChS
17 May 2006	137	0.51	0.28	2.69	1.05	4.29	1	0.62	0.29	4.12	1.84	7.06	1
18 May 2006	138	0.10	0.00	4.30	0.88	5.97	1	0.67	0.31	10.56	2.54	19.22	1
2 Jun 2006	153	0.10	0.00	4.59	0.91	6.37	1	0.10	0.00	3.83	0.77	5.31	1
4 Jun 2006	155	0.29	0.19	2.98	0.95	4.41	1	0.54	0.28	3.62	1.96	5.96	1
8 Jun 2006	159	0.16	0.03	5.81	1.31	8.29	1	0.37	0.23	3.68	1.17	5.67	1
10 Jun 2006	161	0.15	0.08	3.77	0.84	5.33	1	0.53	0.25	8.51	2.41	14.43	1
11 Jun 2006	162	–	–	–	–	–	1	–	–	–	–	–	1
15 Jun 2006	166	0.41	0.24	3.51	0.93	5.48	1	0.63	0.33	2.83	1.11	4.74	1
17 Jun 2006	168	0.10	0.00	5.58	0.83	7.76	1	0.10	0.00	6.42	1.10	8.94	1
18 Jun 2006	169	0.34	0.16	6.13	1.73	9.47	1	0.38	0.22	9.01	2.86	14.28	1
20 Jun 2006	171	0.10	0.00	4.19	1.23	5.81	1	–	–	–	–	–	1
30 Jun 2006	181	0.58	0.26	8.82	2.45	15.32	1	0.22	0.13	4.48	1.17	6.53	1
1 Jul 2006	182	0.42	0.27	2.55	1.27	3.92	1	0.21	0.14	3.15	0.85	4.54	1
5 Jul 2006	186	0.10	0.00	3.71	0.75	5.14	1	0.21	0.12	4.89	1.40	7.11	1
6 Jul 2006	187	0.24	0.13	3.58	1.42	5.23	1	0.32	0.17	9.55	3.10	14.74	1
9 Jul 2006	190	0.35	0.09	11.71	2.46	18.38	1	–	–	–	–	–	1
11 Jul 2006	192	0.10	0.00	8.00	1.32	11.15	1	0.10	0.00	6.23	0.97	8.67	1
14 Jul 2006	195	–	–	–	–	–	1	0.10	0.00	5.90	1.19	8.21	1
15 Jul 2006	196	0.33	0.15	9.07	2.35	14.05	1	0.16	0.08	3.97	0.90	5.64	1
18 Jul 2006	199	0.16	0.07	4.43	1.01	6.30	1	0.41	0.19	9.77	2.57	15.72	1
19 Jul 2006	200	0.16	0.07	6.51	1.68	9.31	1	0.59	0.32	2.65	1.58	4.34	1
20 Jul 2006	201	–	–	–	–	–	1	–	–	–	–	–	1
21 Jul 2006	202	0.34	0.20	5.56	1.63	8.57	1	1.01	0.34	11.93	2.32	25.58	1
25 Jul 2006	206	–	–	–	–	–	1	0.19	0.01	4.60	1.66	6.63	1
26 Jul 2006	207	0.22	0.04	7.55	2.06	11.10	1	–	–	–	–	–	1
27 Jul 2006	208	0.10	0.00	4.49	0.81	6.23	1	0.23	0.09	4.15	1.08	6.07	1
28 Jul 2006	209	0.34	0.16	6.10	1.53	9.42	1	0.31	0.15	4.42	1.21	6.69	1
29 Jul 2006	210	0.54	0.23	8.45	2.43	14.40	1	–	–	–	–	–	1
31 Jul 2006	212	–	–	–	–	–	1	0.23	0.13	4.62	1.27	6.77	1
2 Aug 2006	214	–	–	–	–	–	1	0.77	0.26	24.53	4.51	47.51	1
7 Aug 2006	219	0.13	0.06	3.61	0.97	5.06	1	0.10	0.00	5.37	1.07	7.47	1
11 Aug 2006	223	0.53	0.24	9.40	3.34	15.98	1	–	–	–	–	–	1
19 Aug 2006	231	0.10	0.00	4.83	1.03	6.71	1	0.10	0.00	4.72	0.96	6.56	1
23 Aug 2006	235	0.10	0.00	5.17	1.12	7.19	1	0.10	0.00	4.41	0.78	6.12	1
24 Aug 2006	236	–	–	–	–	–	1	–	–	–	–	–	1
29 Aug 2006	241	–	–	–	–	–	1	–	–	–	–	–	1
30 Aug 2006	242	0.10	0.00	6.24	1.08	8.69	1	0.14	0.02	4.56	1.09	6.44	1
31 Aug 2006	243	–	–	–	–	–	3	–	–	–	–	–	3

Table 1. cont'd

		S_0-										
Date (dd month yyyy)	DOY	K–(nm^{-1})	MAD K–(N m^{-1})	S_0–(@ 2 nm)	MAD S_0-	(@ 1.5 nm)	ChS	K+ nm^{-1}	MAD K+ (nm^{-1})	S_0+ @ 2 (nm)	MAD S_0+	S_0+ (@ 1.5 nm)	ChS
2 Sep 2006	245	1.50	0.40	−0.46	1.56	−2.62	1	–	–	–	–	–	1
10 Sep 2006	253	0.16	0.01	5.53	1.12	7.89	1	0.10	0.00	4.45	0.88	6.18	1
14 Sep 2006	257	–	–	–	–	–	0	–	–	–	–	–	0
15 Sep 2006	258	0.57	0.30	2.40	0.91	3.87	0	0.99	0.46	0.91	1.27	1.23	0
16 Sep 2006	259	0.10	0.00	4.94	1.02	6.86	1	0.95	0.20	16.58	1.86	34.83	1
20 Sep 2006	263	0.34	0.23	2.83	1.16	4.26	1	0.84	0.33	3.29	3.29	6.06	1
21 Sep 2006	264	0.33	0.19	3.19	0.99	4.81	1	0.76	0.38	3.15	1.26	5.60	0
Max		2.48	0.56	28.70	3.63	88.81		2.00	0.65	66.81	5.23	190.07	
Min		0.10	0.00	−0.46	0.59	−2.76		0.10	0.00	−8.61	0.52	−27.15	
Mean		0.43	0.17	4.88	1.33	8.38		0.56	0.21	6.34	1.72	12.27	
Median		0.32	0.16	3.66	1.12	5.65		0.48	0.24	4.44	1.42	6.42	

In the charging state column (ChS) 1 stands for overcharged, −1 undercharged, 0 steady-state and 3 not determined. Rejected fitting parameters, for example, due to large K values are indicated with a "–".

negative and positive contributions together. In this study, the contribution was calculated at 2 nm.

By assuming a stationary-state charged fraction of 0.83% for negatively charged particles and a corresponding value of 0.75% for positively charged particles at 2.0 nm (Wiedensohler, 1988; Hoppel and Frick, 1986), it is possible to calculate the ion-induced contribution during new-particle formation events. The total ion-induced contribution was calculated by adding the negative and positive contributions together. In this study, the contribution was calculated at 2 nm.

For all events with a value of $K \leq 1$ (60 and 46 for negatively and positively charged particles, respectively), the median ion-induced contribution was found to be around 6.4% with a median MAD of 1.9% (7.6% at 1.5 nm). For overcharged events only (49 negative and 36 positive events) the median ion-induced contribution was around 6.9% with a median MAD of 2.0%. On the other hand, the median ion-induced contribution for steady-state and undercharged events (11 negative and 9 positive events) was around 3.1% with a median MAD of 1.8%. The latter can be explained by the difficulty in fitting the kind of steady-state events that lead to unjustified high values of the charging state although the value of K is smaller than 1. This only confirms that fitting of steady-state events is difficult.

All of the median values given above were calculated by adding the median negative ion-induced contribution to the median positive ion-induced contribution. By limiting our analysis to the events for which both negative and positive values of K were below 1 nm^{-1}, a higher ion-induced contribution (7.2%) was obtained because overcharged events are fitted more easily. The ion-induced contribution at 2.0 nm of a perfectly steady-state event would be around 1.6% (1.6% of 2 nm particles are charged; Wiedensohler, 1988).

3.3. Seasonal analysis of the fitting parameters

In Fig. 7, one can see the fitted parameters for all event days for which $K \leq 1$ as a function of the day of the year. The value of K had a tendency to be higher for undercharged and steady-state events than for overcharged events for both negatively and positively charged particles. As expected, the value of S_0 was higher for overcharged events than for undercharged events. The high values of K presented in Table 1 for negative particles in spring were probably due to slightly overcharged particles behaving like steady-state events (only the smallest size bin is significantly over the steady-state and the fit tends to bend at only one size, this leads to a high values for K and S_0). Really steady-state events and the latter type of event cannot be distinguished one from another. As observed from the classification of event days (Fig. 5), undercharged and steady-state events tended to happen during winter while only overcharged events were seen in summer. The median ion-induced nucleation contribution in summer (June–August) was of 7.6% with a median MAD of 1.8% while the contribution fell to 4.9% (median MAD of 1.9%)

Table 2. Median values of the parameters K and S_0 and its median MAD (median absolute deviation) in parenthesis

		Negative		Positive	
		Median K (nm^{-1})	Median S_0	Median K (nm^{-1})	Median S_0
All K	Over	0.28 (0.13)	4.3 (1.12)	0.34 (0.19)	4.6 (1.53)
	Under	1.2 (0.56)	−0.04 (1.25)	0.71 (0.33)	0.72 (1.43)
	s-s	0.5 (0.26)	2.43 (1.01)	0.76 (0.32)	2.34 (1.27)
	All	0.32 (0.16)	3.66 (1.12)	0.48 (0.24)	4.44 (1.42)
$K <= 1$	Over	0.24 (0.12)	4.3 (1.12)	0.31 (0.15)	4.48 (1.39)
	Under	–	–	0.59 (0.27)	0.52 (1.42)
	s-s	0.42 (0.24)	2.4 (0.97)	0.66 (0.29)	2.34 (1.26)
	all	0.29 (0.14)	3.74 (1.06)	0.37 (0.20)	4.37 (1.33)

For negatively and positively charged particles and for each charging state class. All these values have been calculated for $d_0 = 2$ nm.

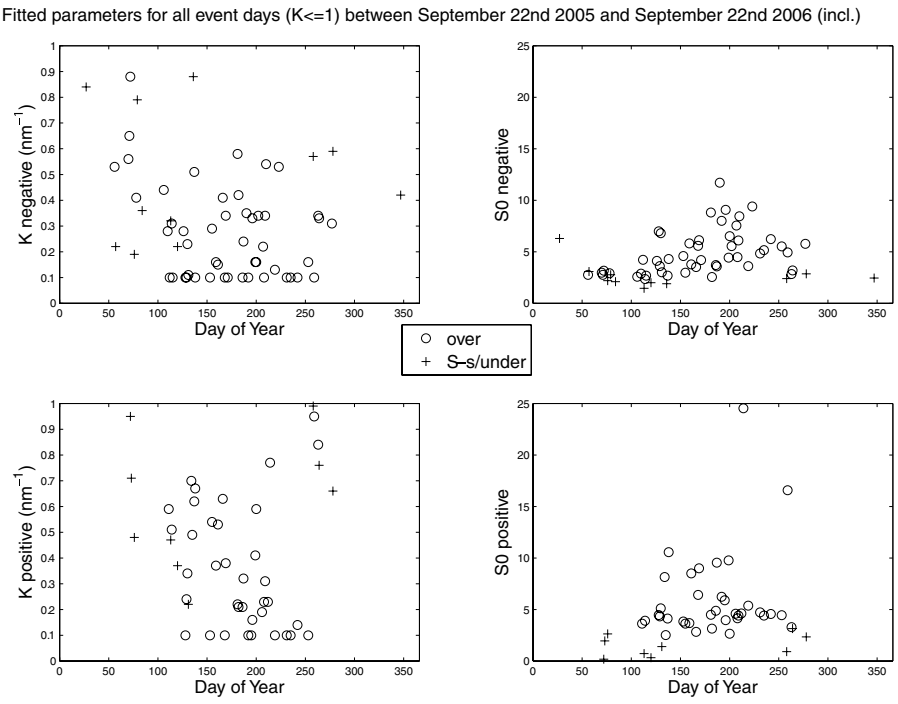

Fig. 7. The K and S_0 parameters are plotted as a function of time of year for overcharged ('over', red) and steady-state ('s-s')/undercharged ('under', blue) events and for negatively (up) and positively (down) charged particles. The data are based on Table 1, S_0 is the value at 2 nm, $K \leq 1$.

during both spring and autumn (March–May and September–November).

The correlation of total ion-induced contribution with (1) temperature; (2) relative humidity and (3) the formation rate at 3 nm J_3 (DMPS; Riipinen et al., 2007) were studied. In all three cases, the correlation coefficient was very low (0.08, 0.02 and 0.1, respectively).

4. Conclusions

In this work, one year of Ion-DMPS measurement data was presented and analysed. New-particle formation events were classified for the whole year according to measured particle charging states. 'Undercharged' and 'steady-state' events were mostly happening around winter, whereas 'overcharged' events dominated clearly during the warmer season. The IIC was higher during summer than during the rest of the year (2.7% difference). During this whole year, overcharged events were the most frequent ones.

The median charging state of all the events with a parameter $K \leq 1$ was 3.7 and 4.4 for negatively and positively charged particles, respectively. This resulted in a median ion-induced contribution of 6.4% (median MAD of 1.9%) to the total particle formation rate at 2 nm, knowing that the steady state charged

fraction of particles at this size is around 1.6% (Wiedensohler, 1988). The contribution of ion-induced nucleation exceeded 10% in only a few new-particle formation days, and no days with dominant contribution from ion-induced nucleation was found during the study period.

The analytical equation describing the charging state of a growing nucleation mode (Kerminen et al., 2007) used in our analysis was found reliable in most situations. However, in some of the cases where the memory of the initial formation mechanism had been lost during the particle growth or when the nucleation was happening at steady-state, misleading results were obtained.

The Ion-DMPS with its theoretical background provides useful tool for getting information about the contribution of ion-induced nucleation. The device would provide even more specific information if analysed separately during different time periods of the days. This, however, was not investigated in the current work.

5. Acknowledgments

Pasi Aalto and the staff of the SMEAR II station are gratefully acknowledged for their maintenance work on the ion-DMPS during the measurements. The Maj and Tor Nessling Foundation is acknowledged for its support in this project. The referees are acknowledged for their constructive comments that have improved this manuscript.

References

Chung, C. E., Ramanathan, V., Kim, D. and Podgorny, I. A. 2005. Global anthropogenic aerosol direct forcing derived from satellite and ground-based observations. *J. Geophys. Res.* **110**, D24207, doi:10.1029/2005JD006356.

Dal Maso, M., Kulmala, M., Riipinen, I., Wagner, R., Hussein, T. and co-authors. 2005. Formation and growth of fresh atmospheric aerosols: eight years of aerosol size distribution data from SMEAR II, Hyytiälä, Finland. *Boreal Environ. Res.* **10**, 323–336.

Donaldson, K., Li, X. Y. and MacNee, W. 1998. Ultrafine (nanometre) particle mediated lung injury. *J. Aerosol Sci.* **29**, 553–560.

Hirsikko, A., Laakso, L., Hõrrak, U., Aalto, P. P., Kerminen, V.-M. and co-authors. 2005. Annual and size dependent variation of growth rates and ion concentrations in boreal forest. *Boreal Environ. Res.* **5**, 357–370.

Hoppel, W. and Frick, G. 1986. Ion-aerosol attachment coefficients and steady-state charge distribution on aerosols in a bipolar environment. *Aerosol. Sci. Technol.* **5**, 1–21.

Iida, K., Stolzenburg, M., McMurry, P., Dunn, M., Smith, J. and co-authors. 2006. Contribution of ion-induced nucleation to new particle formation: methodology and its application to atmospheric observations in Boulder, Colorado. *J. Geophys. Res.* **111**, D23201, doi: 10.1029/2006JD007167.

Kerminen, V.-M., Anttila, T., Petäjä, T., Laakso, L., Gagné, S. and co-authors. 2007. Charging state of the atmospheric nucleation mode: implications for separating neutral and ion-induced nucleation. *J. Geophys. Res.* **112**, D21205, doi:10.1029/2007JD008649.

Kulmala, M.. 2003. How particles nucleate and grow. *Science* **302**, 1000–1001.

Kulmala, M., Vehkamäki, H., Petäjä, T., Dal Maso, M., Lauri, A. and co-authors. 2004. Formation and growth rates of ultrafine atmospheric particles: a review of observations. *J. Aerosol Sci.* **35**, 143–176.

Kulmala, M., Riipinen, I., Sipilä, M., Manninen, H. E., Petäjä, T. and co-authors. 2007. Toward direct measurment of atmospheric nucleation. *Science* **318**, 89–92.

Laakso, L., Gagné, S., Petäjä, T., Hirsikko, A., Aalto, P. P. and co-authors. 2007. Detecting charging state of ultra-fine particles: instrumental development and ambient measurements. *Atmos. Chem. Phys.* **7**, 1333–1345.

Lohmann, U. and Feichter, J. 2005. Global indirect aerosol effects: a review. *Atmos. Chem. Phys.* **5**, 715–737.

Mäkelä, J. M., Salm, J., Smirnov, V. V., Koponen, I., Paatero, J. and co-authors. 2003. Electrical charging state of fine and ultrafine particles in boreal forest air. *J. Aerosol Sci.* **32**, S149–150.

Penner, J. E., Quaas, J., Storelvmo, T., Takemura, T., Boucher, O. and co-authors. 2006. Model intercomparison of indirect aerosol effects. *Atmos. Chem. Phys.* **6**, 3391–3405.

Pope, C. A., III and Dockery, D. W. 2006. Health effects of fine particulate air pollution: lines that Connect. *J. Air Waste Manage. Assoc.* **56**, 709–742.

Reischl, G. P., Mäkelä, J. M., Karch, R. and Necid, J. 1996. Bipolar charging of ultrafine particles in the size range below 10 nm. *J. Aerosol. Sci.* **27**, 931–949.

Riipinen, I., Sihto, S.-L., Kulmala, M., Arnold, F., Dal Maso, M. and co-authors. 2007. Connections between atmospheric sulphuric acid and new particle formation during QUEST III-IV campaigns in Heidelberg and Hyytiälä. *Atmos. Chem. Phys.* **7**, 1899–1914.

Seinfeld, J. H. and Pandis, S. N. 1998. *Atmospheric Chemistry and Physics: From Air Pollution to Climate Change*. Wiley, New York.

Spracklen, D. V., Carslaw, K., Kulmala, M., Kerminen, V.-M., Mann, G. W. and co-authors. 2006. The contribution of boundary layer nucleation events to total particle concentrations on regional and global scales. *Atmos. Chem. Phys.* **6**, 5631–5648.

Stolzenburg, M. and McMurry, P. 1991. An ultrafine aerosol condensation nucleus counter. *Aerosol Sci. Technol.* **14**, 48–65.

Tammet, H. 2006. Continuous scanning of the mobility and size distribution of charged clusters and nanometer particles in atmospheric air and the Balanced Scanning Mobility Analyzer BSMA. *Atmos. Res.* **82**, 523–535.

Twomey, S. 1991. Aerosols, clouds and radiation. *Atmos. Environ.* **25A**, 2435–2442.

Vana, M., Tamm, E., Hõrrak, U., Mirme, A., Tammet, H. and co-authors. 2006. Charging state of atmospheric nanoparticles during the nucleation burst events. *Atmos. Res.* **82**, 536–546.

Wiedensohler, A. 1988. An approximation of the bipolar charge distribution for particles in the submicron range. *J. Aerosol Sci.* **19**, 387–389.

Winklmayr, W., Reischl, G., Lindner, A. and Berner, A. 1991. A new electromobility spectrometer for the measurement of aerosol size distributions in the size range from 1 to 1000 nm. *J. Aerosol Sci.* **22**, 289–296.

Yu, F. and Turco, R. 2001. From molecular clusters to nanoparticles: role of ambient ionization in tropospheric aerosol formation. *J. Geophys. Res.* **106**, 4797–4817.

Yu, F., Wang, Z., Luo, G. and Turco, R. 2006. Ion-mediated nucleation as an important global source of tropospheric aerosols. *Atmos. Chem. Phys. Dicuss.* **7**, 13597–13626.